

Identification and Distribution of the Interstitial Cells of Cajal in the Abomasum of Goats

Cell Transplantation
2018, Vol. 27(2) 335-344
© The Author(s) 2017
Reprints and permission:
sagepub.com/journalsPermissions.nav
DOI: 10.1177/0963689717722561
journals.sagepub.com/home/ccl


Lingling Wang¹, Yu Liang¹, Qiusheng Chen¹,
Nisar Ahmed¹, Feng Wang², Bing Hu³, and Ping Yang^{1,2}

Abstract

The interstitial cells of Cajal (ICCs) are regarded as pacemakers and are involved in neurotransmission in the gastrointestinal tract (GIT) of animals. However, limited information is available about the existence of ICCs within the GIT of ruminants. In this study, we investigated the ultrastructural characteristics and distribution of ICCs in goat abomasum using transmission electron microscopy and c-kit immunohistochemistry. Two different kinds of c-kit immunoreactive cells were observed in the abomasum. The first was identified as ICCs, which appeared to be multipolar or bipolar in shape, with some processes. These c-kit immunoreactive cells were deposited in the submucosal layer, myenteric plexus between the circular and longitudinal muscle layers, and within the longitudinal and circular muscle layers of the abomasum. The second type of cell was round in shape and was identified as mast cells, which were located in the submucosal layer as well as in the lamina propria. Ultrastructurally, ICCs were also observed as stellate or spindle-shaped cells, which were consistent in shape with our c-kit immunoreactive cells. In the cytoplasm of ICCs, numerous mitochondria, rough endoplasmic reticulum, and caveolae were detected. ICCs were located in the myenteric plexus between the longitudinal and circular muscle layers (ICC-MY), with the longitudinal and circular muscle layer was replaced as “intramuscular layers” (ICC-IM), and in the submucosal layer (ICC-SM). In addition, we found ICCs surrounding nerve fibers and smooth muscle cells, where they formed heterocellular junctions in the form of close membrane associations or gap junctions and homocellular junctions among the processes of the ICCs. In the current study, we provide the first complete characterization of ICCs within the goat abomasum and propose that ICCs might have a key role in producing contractions in the ruminant stomach for proper absorption of nutrients.

Keywords

identification, interstitial cells of Cajal, abomasum, goat

Introduction

During the last few decades, the interstitial cells of Cajal (ICCs) were identified as a component of the gastrointestinal tracts (GITs) in several species^{1,2}. ICCs appear multipolar (dendritic-like) or bipolar in shape, with various cytoplasmic organelles, and have a discontinuous basal lamina. However, the existence of caveolae in the processes of the ICCs is one of their key identifying features. A subpopulation of ICCs is regarded as pacemaker cells that can generate electrical slow waves³⁻⁸. The other populations are thought to be the key to transducing neurotransmissions by regulating input from enteric motor neurons⁹⁻¹⁵. The recognition of its physiological function has led researchers to study ICCs in various organs, such as the GIT of different animals and humans¹⁶⁻¹⁹. Recently, it has been reported that any damage or loss of the ICC network may lead to disorders of the GIT^{20,21}.

c-kit, a tyrosine kinase receptor, is considered to be a reliable immunochemical marker for ICC identification and location in various organs²²⁻²⁴. While the c-kit protein can

¹ College of Veterinary Medicine, Nanjing Agricultural University, Nanjing, People's Republic of China

² College of Animal Science & Technology, Nanjing Agricultural University, Nanjing, People's Republic of China

³ College of Life Sciences, Nanjing Agricultural University, Nanjing, People's Republic of China

Submitted: April 14, 2017. Revised: May 27, 2017.

Accepted: June 20, 2017.

Corresponding Author:

Ping Yang, College of Veterinary Medicine, Nanjing Agricultural University, Nanjing 210095, People's Republic of China.
Email: yangping@njau.edu.cn



also mark mast cells, they are easily differentiated from ICCs according to their morphological characteristics and distribution^{25,26}. ICCs have multipolar (dendritic-like) or bipolar shapes and are present at different locations, such as at the myenteric plexus between the circular and longitudinal muscle layers, intramuscular layer, and submucosal layer. However, mast cells mainly occur in the submucosal layer as well as in the lamina propria and have a round shape. c-kit is a vital member of the protein tyrosine kinase family and it is a stem cell factor ligand. c-kit protein expression is the key to identifying ICCs and its phenotype conservation. The use of antibodies to neutralize c-kit function and the use of c-kit mutant animals have proven valuable in determining the physiological role of ICCs²⁷. However, transmission electron microscopy (TEM) still remains the gold standard for the identification of ICCs. The ultrastructural characteristics of ICCs are present in different mammals, such as rabbits, pigs, dogs, and humans²⁸, but no attention has been paid to them in ruminants. Most studies of ICCs have been limited primarily to common laboratory mammals and humans.

Ruminants have 4-chambered stomachs. The first 3 chambers, the rumen, reticulum, and omasum, are collectively named the forestomach. The fourth chamber is known as the abomasum, which is a glandular part that secretes gastric juice. The abomasum corresponds to the pylorus and is the “true stomach” of ruminants²⁹. The abomasum is a significant part of the ruminant stomach and has a crucial role in the absorption of nutrients, as it is the location where digestion occurs via physical and biochemical processes. In the current study, we investigated, for the first time, the ultrastructural characteristics of ICCs and their distribution in the goat abomasum by TEM and c-kit immunohistochemistry.

Materials and Methods

Ethics Statement

The experimental design and sampling procedures were approved by the Animal Ethics Committee of Nanjing Agricultural University, China, before the start of the current experiment. The experiment was conducted according to the “Guidelines on Ethical Treatment of Experimental Animals” by the Jiangsu Provincial People’s Government (SYXK (SU) 2011-0036).

Materials

Six normal adult goats of either sex were obtained from a commercial farm. Abomasum samples were taken from these goats right after euthanasia. All efforts were made to minimize animal suffering. Samples were immediately washed with 0.1 mol/L phosphate-buffered saline (PBS; pH 7.3), then some samples were fixed in 4% paraformaldehyde (PFA) in 0.1 mol/L PBS overnight and embedded in paraffin wax. Other samples were cut into 1 mm³ blocks and immersed into 2.5% glutaraldehyde in 0.1 mol/L PBS overnight.

Immunohistochemistry

Tissue was sectioned (6 μm) and stained using standard immunohistochemical techniques for microstructure analysis. Samples underwent deparaffinization in an ethanol gradient, followed by washing in PBS; endogenous peroxidase activity was blocked with 3% hydrogen peroxide in PBS for 15 min at 37 °C. The sections were then covered with 5% bovine serum albumin (BSA). The sections were incubated with rabbit anti-c-kit (1:100) antibody (Boster Bio-Technology, Wuhan, China) and rabbit anti-tryptase (1:100) antibody (Boster Bio-Technology) overnight at 4 °C, as well as 1 section was incubated with PBS as a control. After incubation with primary antibody, the sections were incubated in biotinylated antirabbit immunoglobulin G secondary antibody (Boster Bio-Technology) for 1 h at 4 °C. The sections were then rehydrated in PBS and incubated with avidin–biotinylated peroxidase complex for 45 min at 37 °C. For color development, peroxidase activity was revealed using 3,3-diaminobenzidine ((DAB) Boster Bio-Technology) under a microscope.

TEM

The blocks of samples were submerged in 1% osmium tetroxide in the 0.1 mol/L PBS (pH 7.3) for 60 min. The blocks were dehydrated in ascending concentrations of ethyl alcohol, infiltrated with a propylene oxide–Araldite mixture, and embedded in Araldite. Ultrathin sections (50 nm) were stained with 1% uranyl acetate and lead citrate for 20 min each.

Equipment

For light microscopy, the sections were examined and photographed using an Olympus DP73 microscope (Guangzhou City, Guangdong Province, China). For TEM, the sections were examined and photographed with an H-7650 transmission electron microscope (Hitachi Suzhou City, Hong Kong Village 58, Room 602).

Results

Localization of c-Kit Immunoreactive Cells in the Goat Abomasum

In the present study, we observed 2 types of c-kit immunoreactive cells. One group of c-kit immunoreactive cells appeared multipolar (dendritic-like) or bipolar in shape and was identified as ICCs (Fig. 1a–d). The fusiform cell body was observed in the submucosal border with 2 processes at each pole (Fig. 1a). c-kit immunoreactive cells were located in the 3 different regions of the abomasum: along with the submucosal layer (ICC-SM) (Fig. 1a), in the myenteric plexus between the circular and longitudinal muscle layers (ICC-MY) (Fig. 1b), and within the longitudinal and circular muscle layers of the abomasum (ICC-IM) (Fig. 1c). In

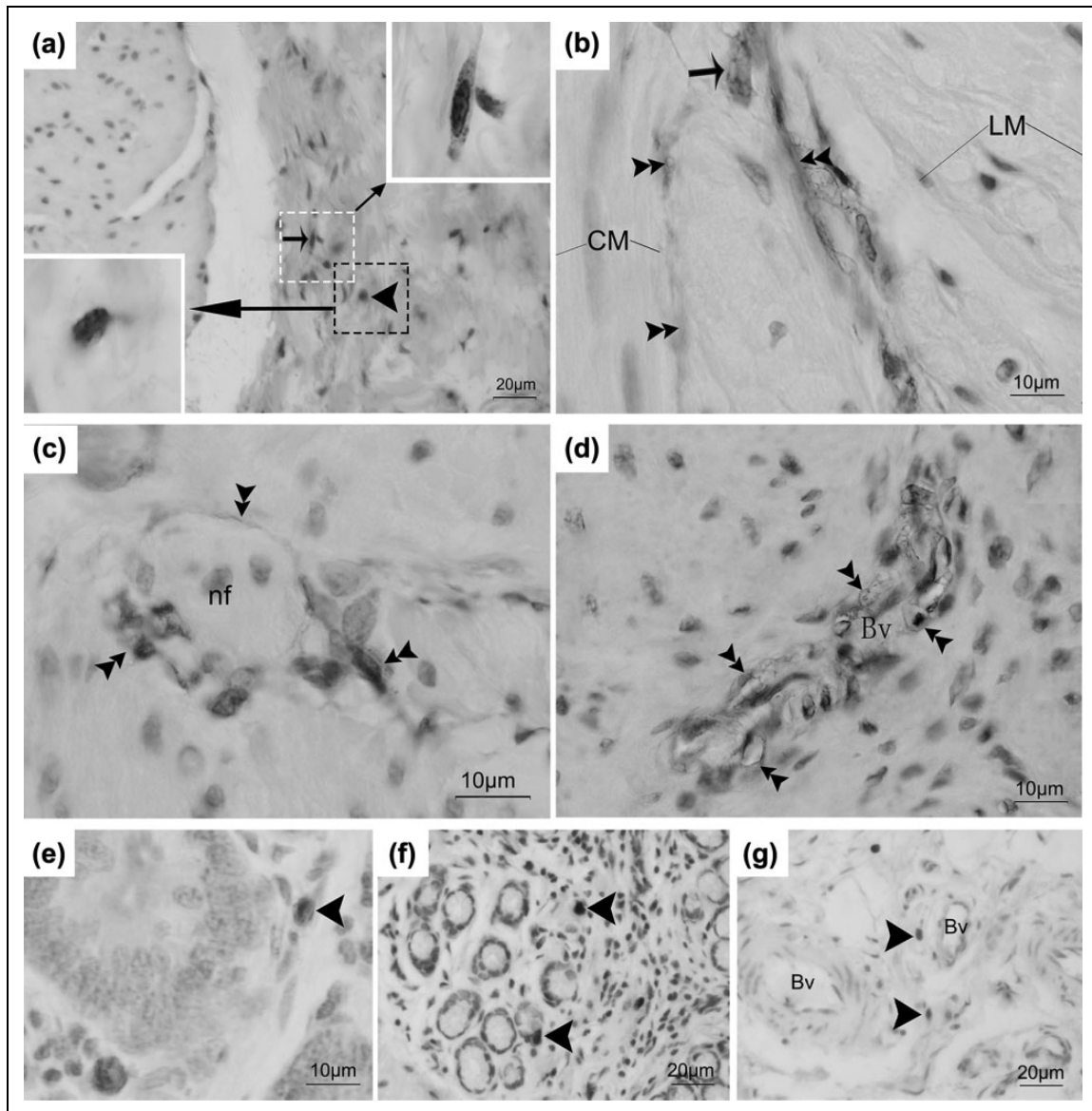


Fig. 1. Light micrograph showing c-kit immunoreactive cells and tryptase immunoreactive cells in the abomasum. (a) The c-kit immunoreactive cells were seen in the submucosal border. (b) A multipolar (dendritic-like)-shaped cells (arrow) and the long process of c-kit immunoreactive cells (double arrowheads) were found in the myenteric plexus between the circular and longitudinal muscle layers. (c) and (d) The process of intramuscular c-kit immunoreactive cells (double arrowheads) surrounded never fibers and blood vessels. (e) The c-kit immunoreactive cells (arrowhead) were located in the lamina propria. (f) The tryptase immunoreactive cells (arrowhead) were deposited in the lamina propria. (g) A few tryptase immunoreactive cells (arrowhead) near to blood vessel in the submucosal border. The small arrow represents interstitial cells of Cajal; arrowhead represents mast cell; double arrowhead represents the process of ICCs. nf, nerve fiber; Bv, blood vessel; LM, the longitudinal muscle layer; CM, the circular muscle layer; LP, the lamina propria. Bar = 20 μ m (a, f, and g); bar = 10 μ m (b, c, d, and e).

addition, we found that c-kit immunoreactive cells always surrounded nerve fibers and blood vessels (Fig. 1c, d). Another group of round-shaped cells was found and identified as mast cells (Fig. 1a and e). These cells were mostly located in the submucosal layer as well as in the lamina propria of the abomasum (Fig. 1a and e). An antibody against tryptase protein was chosen as special maker for mast cells. Tryptase immunoreactive cells appeared as round shaped. These cells were mainly deposited in the lamina propria and also close to the blood vessel in the submucosal

layer (Fig. 1e and f). The morphology and distribution of tryptase-immunoreactive cells were consistent with c-kit immunoreactive mast cells.

Ultrastructural Characteristics of ICCs in the Goat Abomasum

Morphologically, ICCs were observed to be stellate or spindle-shaped, with some processes (Fig. 2a and b). The nuclei of ICCs were found to be fusiform or irregular in shape and

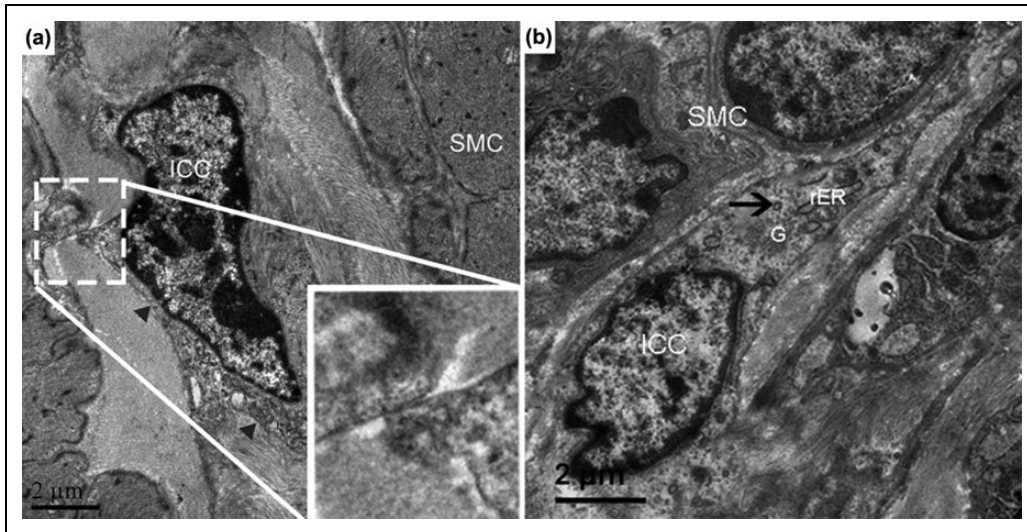


Fig. 2. Transmission electron micrograph showing the general morphological characteristics of ICCs in the abomasum. (a) A stellate-shaped ICC forming networks with another process. Inset: Higher magnification of the boxed area in panel (a). (b) An irregular shaped ICC within intramuscular layer. ICC, interstitial cells of Cajal; SMC, smooth muscle cell; Mi, mitochondria, G, Golgi; (triangle), the discontinuous basal lamina; rER, rough endoplasmic reticulum; arrow, caveolae. Bar = 20 μm (a and b).

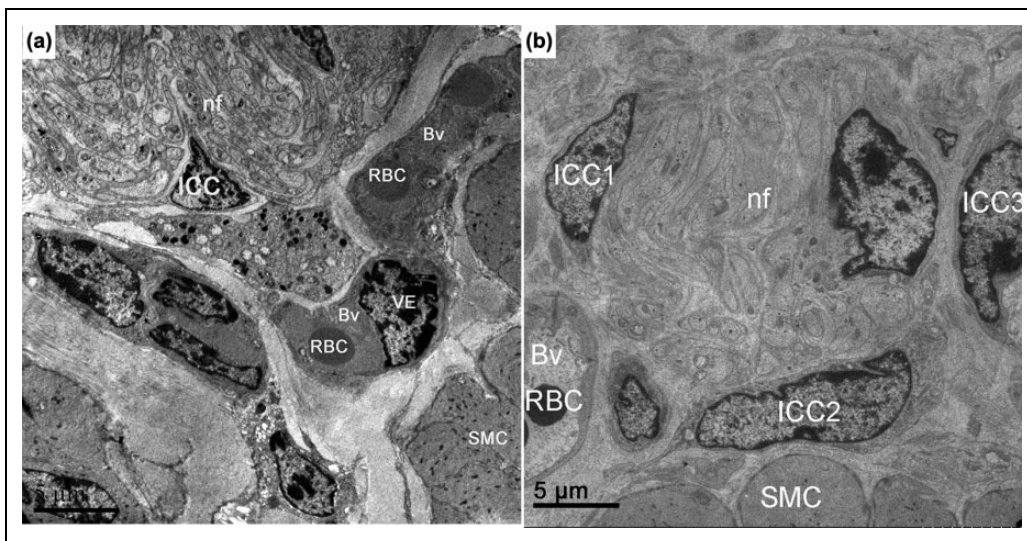


Fig. 3. Transmission electron micrograph showing ICC in the myenteric plexus between the longitudinal and circular muscle layers (ICC-MY) in the abomasum. (a) A triangular shaped ICC embedded in the periphery of the nerve varicosity. (b) ICCs (ICC1, ICC2, ICC3) surrounding nerve fiber. ICC, interstitial cells of Cajal; Mi, mitochondria; SMC, smooth muscle cells; nf, nerve fiber; Bv, blood vessels; VE, vascular endothelial layer; RBC, red blood cell. Bar = 5 μm (a and b).

contained a dense band of marginal heterochromatin. The emergence of the primary process appeared wide with a thin, electron-dense, uniform dendritic process. Cytoplasmic organelles included Golgi complexes, numerous mitochondria, and abundant rough endoplasmic reticulum, and a discontinuous basal lamina was observed. Occasionally, intermediate filaments were also detected in the cytoplasm of ICCs. Meanwhile, caveolae were frequently seen along the plasma membrane, which distinguished these cells from fibroblasts. ICCs formed close contact or distinct gap junctions with neighboring ICCs and smooth muscle cells (SMCs) (Fig. 2a and b).

ICCs were found in close proximity of myenteric plexus between the circular and longitudinal muscle layers, indicating the presence of one of the subtypes of ICCs, named ICC-MY (Fig. 3a and b). The ICCs with triangular nuclei were embedded in the periphery of the nerve varicosity, and the processes of ICCs surrounded the blood vessel. Meanwhile, long processes of the ICCs formed gap junctions with SMCs (Fig. 3a). ICC-MY were stellate or spindle in shape, with 2 main processes that generally had long, slender, or dendritic characteristics. Two to 5 of these cells were found around the bundle of nerve fibers (Fig. 3b).

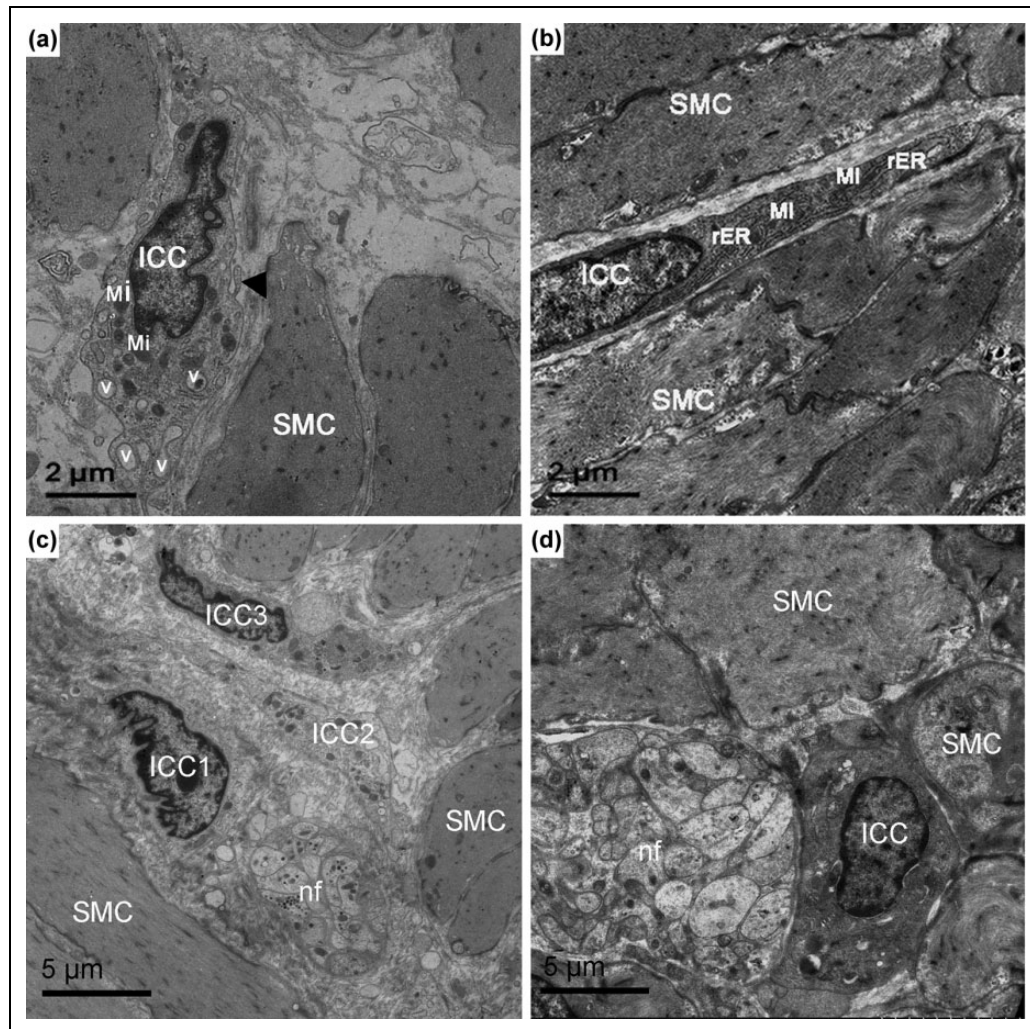


Fig. 4. Intramuscular ICC (ICC-IM) contact with SMC and nerve fibers. (a) A stellate-shaped multipolar ICC. (b) A spindle-shaped ICC with 2 long processes, traversing between SMC. (c) A spindle-shaped ICC forming synaptic-like varicosity with nerve terminals. (d) A round-shaped ICC forming typical contacts with SMC and nerve fibers structure. ICC, interstitial cell of Cajal; SMC, smooth muscle cells; nf, nerve fiber; arrow, the processes of ICC; V, vesicle; Mi, mitochondria; rER, rough endoplasmic reticulum; triangle, caveolae. Bar = 2 μm (a and b); bar = 5 μm (c and d).

ICCs were also observed within the circular and longitudinal muscle layers (Figs. 4a–d, 5a, and 6a), which were regarded as intramuscular ICCs (ICC-IM). The ultrastructure of ICC-IM contained cytoplasmic organelles, such as numerous mitochondria, rough endoplasmic reticulum, and intermediate filaments, as well as an incomplete basal lamina (Fig. 4a). Spindle-shaped ICC-IM have 2 long processes (Fig. 4b). ICC-IM were also associated with intimate synaptic-like varicosity nerve terminals (Fig. 4c and d), which contained both large and dense core vesicles and small electron lucent vesicles. At regions of close contact, electron-dense areas were observed along the pre- and postjunctional membrane and within the membranes of the nerve terminals and ICCs. There was also distinct electron-dense material in the extracellular space between the nerve terminals and ICCs (Fig. 4d). The processes of the ICCs imbedded in the SMCs (Fig. 4c). The ICC-IM showed a stellate shape with multiple

cytoplasmic processes, which formed gap junctions with adjacent SMCs (Fig. 5a–d). Another type of junction was observed between ICCs and SMCs, which was named peg-and-socket-like junction (Fig. 6a and b).

Furthermore, we observed that a few ICCs run along with the submucosal border of circular smooth muscle bundles, which are thought to be ICC-SM. Their cytoplasm contained mitochondria, abundant caveolae, and large quantities of rough endoplasmic reticulum, as well as a distinct basal lamina, and they formed gap junctions with neighboring processes of other ICC-SM. This subtype of ICC had 2 main processes that appeared winding and long (Fig. 7a). A few ICC-SM were also found surrounding blood vessels (Fig. 7b). We also identified fibroblast cells with short processes, which were different from those of ICCs. They were observed with round nuclei and an abundant cytoplasmic area and contained fewer mitochondria and more rough

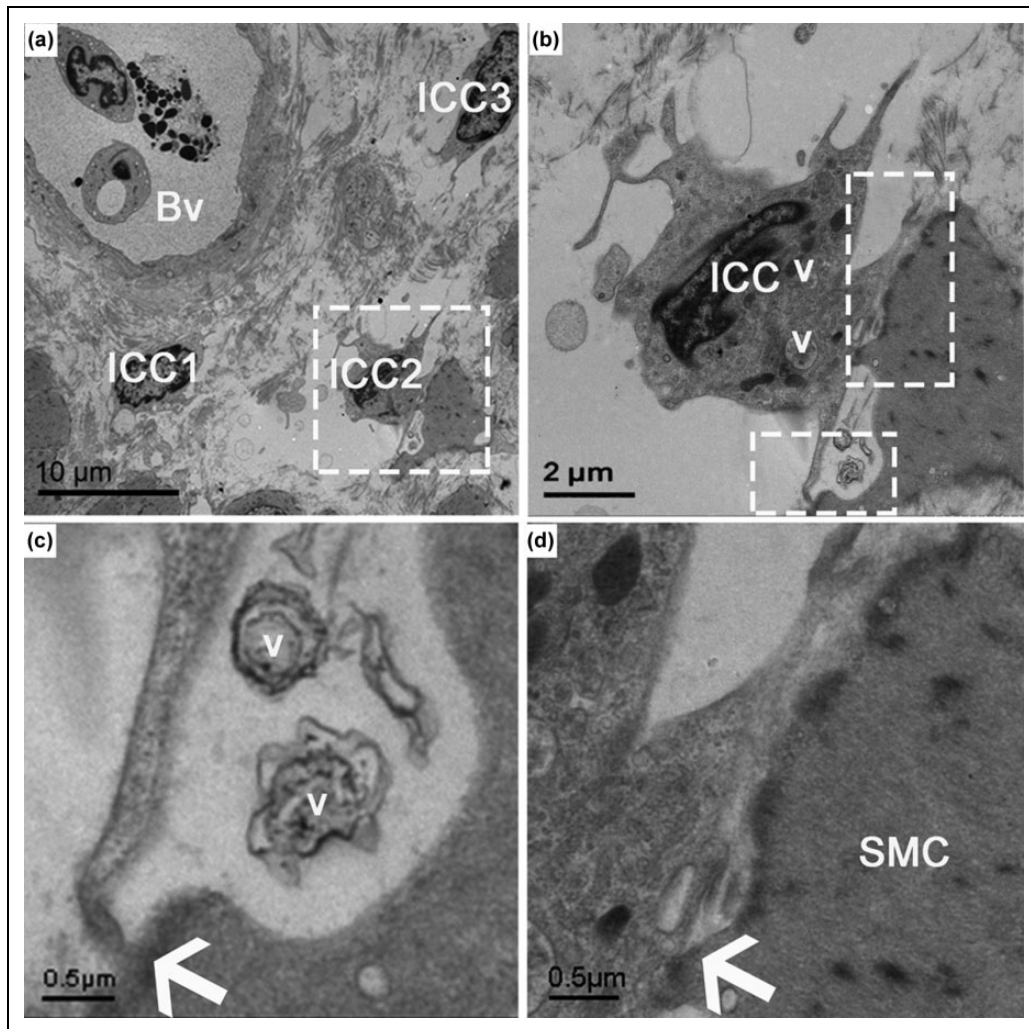


Fig. 5. Transmission electron micrograph showing gap junction between an Intramuscular ICC (ICC-IM) and a SMC. (a) A bundle of ICCs surrounding the blood vessel. (b) Higher magnification of the boxed area in (a), see a stellate-shaped ICC forming gap junction with smooth muscle. (c) and (d) Higher magnification of ICC forming gap junction with the SMC of the boxed area in (b). ICC, interstitial cell of Cajal; SMC, smooth muscle cell; Bv, blood vessel; V, vesicle; Mi, mitochondria; arrow, gap junction. Bar = 10 μm (a); bar = 2 μm (b); bar = 0.5 μm (c and d).

endoplasmic reticula. Caveolae, intermediate filaments, and basal lamina were absent. They did not contact muscle or nerve cells (Fig. 8a and b).

Discussion

This is the first ever study to identify the ultrastructure and distribution of ICCs in the goat abomasum by TEM and c-kit immunohistochemistry. We observed that the morphology of ICCs was similar to those in previous reports on the guinea pig small intestine³⁰, the human GIT³¹, and chicken oviducts³². In previous studies, c-kit protein specifically labeled ICCs in bovines²⁴, rats³³, mice³⁴, and guinea pigs³⁵. Hudson et al³⁶. showed a widespread existence of c-kit immunoreactive cells in all layers of the horse's GIT, including at the level of the myenteric plexus between the circular and longitudinal muscle layers, in the intramuscular layer, in the submucosal layer, and in the lamina propria. Their results

showed that 2 different types of c-kit immunoreactive cells were further confirmed in the present study by light microscopy. One type of c-kit immunoreactive cell was identified with multipolar (dendritic-like) or bipolar cells. Additionally, another type of cell was oval in shape, which has been named mast cells. In the present study, 3 subtypes of ICCs were noted in the goat abomasum, as previously reported in the stomach of guinea pigs³⁵: (1) a high density of ICC-MY was found in the myenteric plexus between the circular and longitudinal muscle layers, (2) ICC-IM integrated intramuscularly, and (3) ICC-SM at the level of the submucosal layer.

Previous studies have reported that ICC-IM were stellate or spindle in shape and existed within the intramuscular layer in the stomachs of guinea pigs³⁵ and humans³⁷. In the present study, the morphology and distribution of ICC-IM are consistent with these reports. Our results showed that close apposition exists between neuronal cells and ICC-IM in the abomasum, which occurs in a similar manner as in the

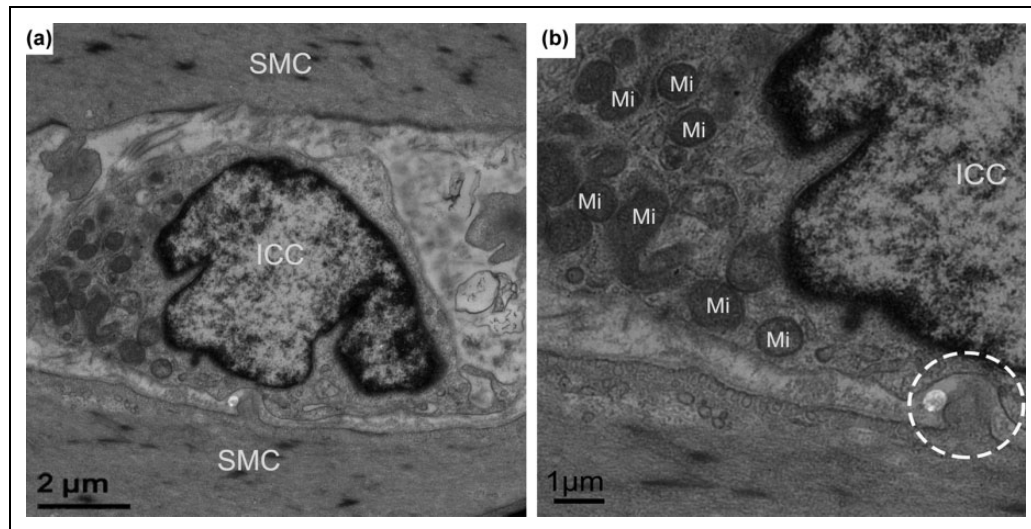


Fig. 6. Another type of contact between Intramuscular ICC (ICC-IM) and SMC: peg-and-socket-like junction. (a) ICC forming peg-and-socket-like junction with SMC. (b) Higher magnification of (a), see the cytoplasmic organelle ICC including rich mitochondria. ICC, interstitial cell of Cajal; SMC, smooth muscle cells; Mi, mitochondria; encircled area, peg-and-socket-like junction. Bar = 2 μm (a); bar = 1 μm (b).

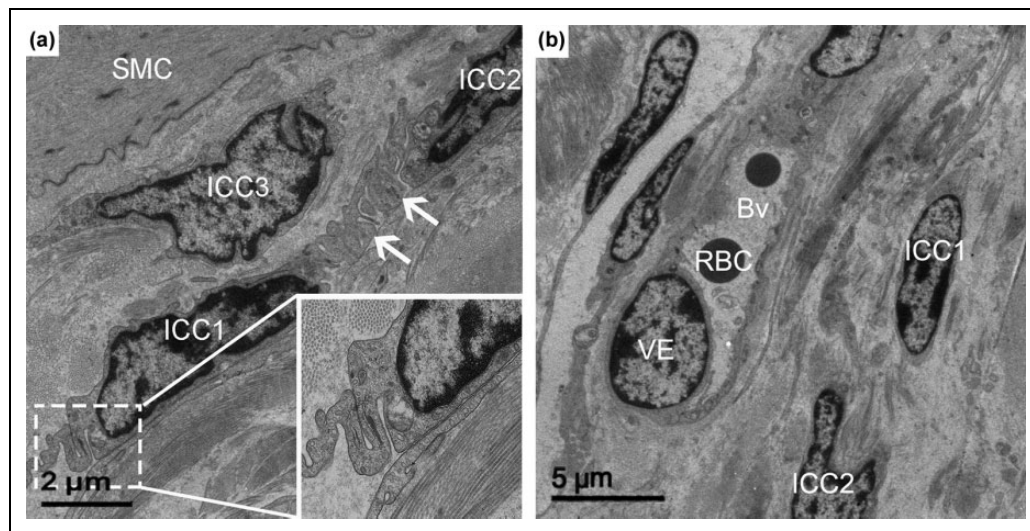


Fig. 7. Transmission electron micrograph showing ICC in the submucosal layers (ICC-SM). (a) The long and winding process of ICCs forming homocellular junctions each other. Inset: Higher magnification of the boxed area in panel (a). (b) A bundle of ICCs surrounding blood vessel. ICC, interstitial cells of Cajal; SMC, smooth muscle cells; arrow, the processes of ICCs; inset, higher magnification of the boxed area in panel a; Bv, blood vessel; RBC, red blood cell; VE, vascular endothelial layer. Bar = 2 μm (a); bar = 5 μm (b).

GIT of guinea pigs¹⁷, canines¹⁸, and mice³⁸, where ICC-IM have been proposed to serve as mediators between the enteric motor neuron and smooth muscles. However, previous studies have documented that this synapse specialization between enteric nerve terminals and SMCs does not exist^{18,38}. Instead, ICC-IM formed gap junctions with adjacent SMCs. The existence of identical relationships between enteric motor cells and ICCs in GIT of the canines and mice, where psychology function is assumed that ICC-IM may be innervated by cholinergic or nitrenergic neurons, indicated a

similar function in the goat stomach. Thus, the present study demonstrated that, as in the canine¹⁸, the neuromuscular junction in the abomasum of goats consists of close contacts between neuronal cells and ICC-IM and regulation of neural inputs through gap junction from ICC-IM to SMCs. We observed synaptic-like junctions with pre- and postjunctional membrane densification occurring between varicose nerve terminals and ICC-IM. Beckett et al³⁸. have identified synapse-like proteins between neurons and ICC-IM in the murine stomach, which suggested that the special structure

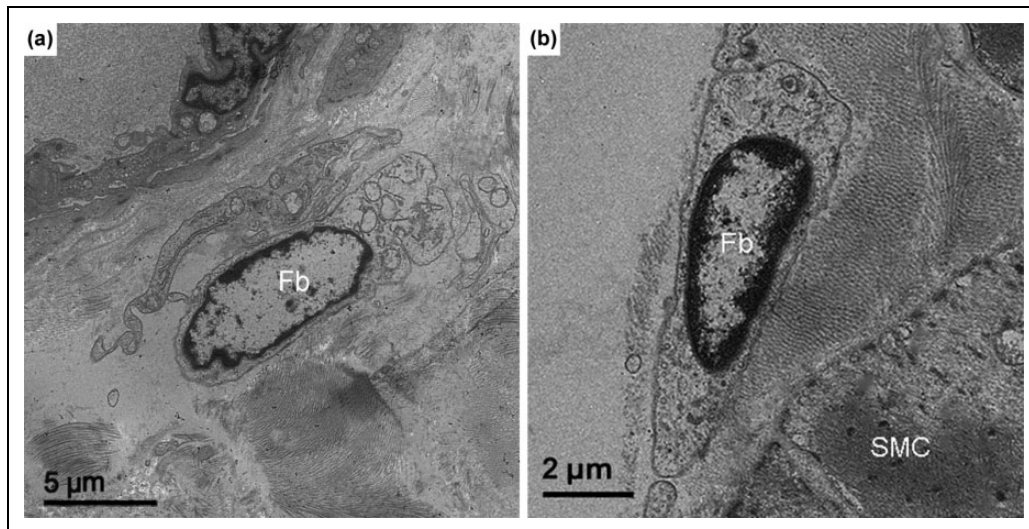


Fig. 8. Transmission electron micrograph showing the fibroblasts in the abomasum. (a) The cytoplasmic organelle of fibroblast including abundant vesicle. (b) Fibroblast near to the SMC. Fb, fibroblast; SMC, smooth muscle cells. Bar = 2 µm (b); bar = 5 µm (a).

was regarded as a primary site of excitatory and inhibitory innervation. The above findings collectively suggested that ICC-IM have excitatory and inhibitory innervations, which might be helpful in the contraction of the ruminant stomach for proper absorption of nutrients.

In the present study, ICC-SM were observed at the submucosal layers of goat abomasum. For their physiological role, it has been reported that ICC-SM can function as a pacemaker in the colon of canines³⁹, humans⁴⁰, and rats⁴¹. Horiguchi et al. proposed that the ICC-SM of canines in the gastric antrum have similar properties to those in the colon⁴². Therefore, the ICC-SM of the stomach can also generate slow waves. The ultrastructure of this type of cell in the rat stomach⁴³, in which ICC-SM were characterized as having cytoplasmic organelles, including abundant mitochondria, rough endoplasmic reticula, and rich intermediate filaments, as well as numerous caveolae and a discontinuous basal lamina. In the present study, we observed the morphology and distribution of ICC-SM are consistent with their studies, so here we hypothesized that the ICC-SM can also generate a slow wave in goat abomasum. Moreover, we found fibroblasts and successfully differentiated them from ICCs. The fibroblasts did not contain basal lamina, caveolae, intermediate filaments, or any visible junctions or contacts with smooth muscles or nerves. In the present study, fibroblasts were distinguished from ICCs, as the former principal did not appear to have gap junctions, intermediate filaments, numerous mitochondria, or basal laminae in the mammalian GIT²⁸.

In summary, in this study, we first investigated ultrastructural characteristics of ICCs by TEM and simultaneously aimed to clarify the distribution of c-kit immunoreactive cells in the goat abomasum. Three classes of ICCs were identified according to TEM and c-kit immunohistochemistry. Two different kinds of c-kit immunoreactive cells were

observed in the abomasum. The first type was ICCs, which appeared multipolar (dendritic-like) or bipolar in shape, while the second type of cells was identified as mast cells and were round in shape. Ultrastructurally, the ICCs were observed to be stellate or spindle in shape, with numerous mitochondria, rough endoplasmic reticula, and many caveolae in the cytoplasm. ICCs were located in the submucosal layer (ICC-SM), myenteric plexus between the circular and longitudinal muscle layers (ICC-MY), and within the longitudinal and intramuscular layers (ICC-IM).

Authors' Note

All data are included in the manuscript and supporting information.

Ethical Approval

This study was approved by the Animal Ethics Committee of Nanjing Agricultural University, China.

Statement of Human and Animal Rights

The experiment was conducted according to the "Guidelines on Ethical Treatment of Experimental Animals" by the Jiangsu Provincial People's Government (SYXK (SU) 2011-0036).

Statement of Informed Consent

There are no human subjects in this article and informed consent is not applicable.

Declaration of Conflicting Interests

The author(s) declared no potential conflicts of interest with respect to the research, authorship, and/or publication of this article.

Funding

The author(s) disclosed receipt of the following financial support for the research and/or authorship of this article: This research was granted and supported by National Natural Science Foundation of China (Youth Project, No. 31402155), the Fundamental Research

Funds for the Central Universities of China (No. Y0201700174), China Postdoctoral Science Foundation Funded Project (No. 2016M591861), the Priority Academic Program Development of Jiangsu Higher Education Institutions, China.

References

- Faussone-Pellegrini MS, Pantalone D, Cortesini C. An ultrastructural study of the interstitial cells of Cajal of the human stomach. *J Submicrosc Cytol Pathol.* 1989;21(3):439–460.
- Junquera C, Martinez-Ciriano C, Castiella T, Serrano P, Aisa J, Calvo E, Lahoz M. Enteric plexus and interstitial cells of Cajal: interrelationship in the stomach of *Podarcis hispanica* (Reptilia). An ultrastructural study. *Histol Histopathol.* 2001;16(3):869–881.
- Sanders KM, Koh SD, Ward SM. Interstitial cells of Cajal as pacemakers in the gastrointestinal tract. *Annu Rev Physiol.* 2006;68:307–343.
- Kito Y, Suzuki H. Properties of pacemaker potentials recorded from myenteric interstitial cells of Cajal distributed in the mouse small intestine. *J Physiol.* 2003;553(Pt 3):803–818.
- Yamataka A, Fujiwara T, Nishiye H, Sunagawa M, Miyano T. Localization of intestinal pacemaker cells and synapses in the muscle layers of a patient with colonic hypoganglionosis. *J Pediatr Surg.* 1996;31(4):584–587.
- Sanders KM. A case for interstitial cells of Cajal as pacemakers and mediators of neurotransmission in the gastrointestinal tract. *Gastroenterology.* 1996;111(2):492–515.
- Huizinga JD, Thuneberg L, Kluppel M, Malysz J, Mikkelsen HB, Bernstein A. W/kit gene required for interstitial cells of Cajal and for intestinal pacemaker activity. *Nature.* 1995;373(6512):347–349.
- Thuneberg L. Interstitial cells of Cajal: intestinal pacemaker cells? *Adv Anat Embryol Cell Biol.* 1982;71:1–130.
- Sanders KM, Salter AK, Hennig GW, Koh SD, Perrino BA, Ward SM, Baker SA. Responses to enteric motor neurons in the gastric fundus of mice with reduced intramuscular interstitial cells of Cajal. *J Neurogastroenterol Motil.* 2014;20(2):171–184.
- Ward SM, Sanders KM. Involvement of intramuscular interstitial cells of Cajal in neuroeffector transmission in the gastrointestinal tract. *J Physiol.* 2006;576(Pt 3):675–682.
- Ward SM, McLaren GJ, Sanders KM. Interstitial cells of Cajal in the deep muscular plexus mediate enteric motor neurotransmission in the mouse small intestine. *J Physiol.* 2006;573(Pt 1):147–159.
- Ward SM, Sanders KM. Interstitial cells of Cajal: primary targets of enteric motor innervation. *Anat Rec.* 2001;262(1):125–135.
- Ward SM. Interstitial cells of Cajal in enteric neurotransmission. *Gut.* 2000;47(Suppl 4):iv40–iv43; discussion iv52.
- Ward SM, Beckett EA, Wang X, Baker F, Khoyi M, Sanders KM. Interstitial cells of Cajal mediate cholinergic neurotransmission from enteric motor neurons. *J Neurosci.* 2000;20(4):1393–1403.
- Burns AJ, Lomax AE, Torihashi S, Sanders KM, Ward SM. Interstitial cells of Cajal mediate inhibitory neurotransmission in the stomach. *Proc Natl Acad Sci U S A.* 1996;93(21):12008–12013.
- Hanani M, Freund HR. Interstitial cells of Cajal—their role in pacing and signal transmission in the digestive system. *Acta Physiol Scand.* 2000;170(3):177–190.
- Wang XY, Sanders KM, Ward SM. Intimate relationship between interstitial cells of Cajal and enteric nerves in the guinea-pig small intestine. *Cell Tissue Res.* 1999;295(2):247–256.
- Horiguchi K, Sanders KM, Ward SM. Enteric motor neurons form synaptic-like junctions with interstitial cells of Cajal in the canine gastric antrum. *Cell Tissue Res.* 2003;311(3):299–313.
- Zhang RX, Wang XY, Chen D, Huizinga JD. Role of interstitial cells of Cajal in the generation and modulation of motor activity induced by cholinergic neurotransmission in the stomach. *Neurogastroenterol Motil.* 2011;23(9):e356–e371.
- Wang XY, Zarate N, Soderholm JD, Bourgeois JM, Liu LW, Huizinga JD. Ultrastructural injury to interstitial cells of Cajal and communication with mast cells in Crohn's disease. *Neurogastroenterol Motil.* 2007;19(5):349–364.
- Zani-Ruttenstock E, Zani A, Paul A, Diaz-Cano S, Ade-Ajayi N. Interstitial cells of Cajal are decreased in patients with gastroschisis associated intestinal dysmotility. *J Pediatr Surg.* 2015;50(5):750–754.
- Isozaki K, Hirota S, Nakama A, Miyagawa J, Shinomura Y, Xu Z, Nomura S, Kitamura Y. Disturbed intestinal movement, bile reflux to the stomach, and deficiency of c-kit-expressing cells in Ws/Ws mutant rats. *Gastroenterology.* 1995;109(2):456–464.
- Han J, Shen WH, Jiang YZ, Yu B, He YT, Li N, Mei F. Distribution, development and proliferation of interstitial cells of Cajal in murine colon: an immunohistochemical study from neonatal to adult life. *Histochem Cell Biol.* 2010;133(2):163–175.
- Marquez SG, Galotta JM, Galvez GA, Portiansky EL, Barbeito CG. Presence of c-kit positive cells in fetal and adult bovine forestomachs. *Biotech Histochem.* 2014;89(8):591–601.
- Romert P, Mikkelsen HB. c-kit immunoreactive interstitial cells of Cajal in the human small and large intestine. *Histochem Cell Biol.* 1998;109(3):195–202.
- Yang P, Yu Z, Gandahi JA, Bian X, Wu L, Liu Y, Zhang L, Zhang Q, Chen Q. The identification of c-kit-positive cells in the intestine of chicken. *Poultry Sci.* 2012;91(9):2264–2269.
- Ward SM, Burns AJ, Torihashi S, Sanders KM. Mutation of the proto-oncogene c-kit blocks development of interstitial cells and electrical rhythmicity in murine intestine. *J Physiol.* 1994;480(Pt 1):91–97.
- Komuro T. Comparative morphology of interstitial cells of Cajal: ultrastructural characterization. *Microsc Res Tech.* 1999;47(4):267–285.
- McGeedy TA, Sack WO. The development of vagal innervation of the bovine stomach. *Am J Anat.* 1967;121(1):121–130.
- Komuro T, Tokui K, Zhou DS. Identification of the interstitial cells of Cajal. *Histol Histopathol.* 1996;11(3):769–786.
- Torihashi S, Horisawa M, Watanabe Y. c-Kit immunoreactive interstitial cells in the human gastrointestinal tract. *J Auton Nerv Syst.* 1999;75(1):38–50.

32. Gandahi JA, Chen SF, Yang P, Bian XG, Chen QS. Ultrastructural identification of interstitial cells of Cajal in hen oviduct. *Poultry Sci.* 2012;91(6):1410–1417.
33. Mitsui R, Komuro T. Distribution and ultrastructure of interstitial cells of Cajal in the gastric antrum of wild-type and Ws/Ws rats. *Anat Embryol (Berl).* 2003;206(6):453–460.
34. Sun X, Yu B, Xu L, Dong W, Luo H. Interstitial cells of Cajal in the murine gallbladder. *Scand J Gastroenterol.* 2006;41(10):1218–1226.
35. Burns AJ, Herbert TM, Ward SM, Sanders KM. Interstitial cells of Cajal in the guinea-pig gastrointestinal tract as revealed by c-kit immunohistochemistry. *Cell Tissue Res.* 1997;290(1):11–20.
36. Hudson NPH, Pearson GT, Kitamura N, Mayhew IG. An immunohistochemical study of interstitial cells of Cajal (jmath) in the equine gastrointestinal tract. *Res Vet Sci.* 1999;66(3):265–271.
37. Radenkovic G, Savic V, Mitic D, Grahovac S, Bjelakovic M, Krstic M. Development of c-kit immunopositive interstitial cells of Cajal in the human stomach. *J Cell Mol Med.* 2010;14(5):1125–1134.
38. Beckett EA, Takeda Y, Yanase H, Sanders KM, Ward SM. Synaptic specializations exist between enteric motor nerves and interstitial cells of Cajal in the murine stomach. *J Comp Neurol.* 2005;493(2):193–206.
39. Serio R, Huizinga JD, Barajas-Lopez C, Daniel EE. Interstitial cells of Cajal and slow wave generation in canine colonic circular muscle. *J Auton Nerv Syst.* 1990;(Suppl 30):S141–S143.
40. Rae MG, Fleming N, McGregor DB, Sanders KM, Keef KD. Control of motility patterns in the human colonic circular muscle layer by pacemaker activity. *J Physiol.* 1998;510(Pt 1):309–320.
41. Pluja L, Alberti E, Fernandez E, Mikkelsen HB, Thuneberg L, Jimenez M. Evidence supporting presence of two pacemakers in rat colon. *Am J Physiol Gastrointest Liver Physiol.* 2001;281(1):G255–G266.
42. Horiguchi K, Semple GS, Sanders KM, Ward SM. Distribution of pacemaker function through the tunica muscularis of the canine gastric antrum. *J Physiol.* 2001;537(Pt 1):237–250.
43. Ishikawa K, Komuro T, Hirota S, Kitamura Y. Ultrastructural identification of the c-kit-expressing interstitial cells in the rat stomach: a comparison of control and Ws/Ws mutant rats. *Cell Tissue Res.* 1997;289(1):137–143.